# A theoretical study of structural and electronic properties of alkaline-earth fluoride clusters

Ratnesh K. Pandey [a,b], Kevin Waters [b], Sandeep Nigam [b,c], Haiying He [d], Subhash S. Pingale [e], Avinash C. Pandey [a,f], Ravindra Pandey [b,*]

[a] Nanotechnology Application Centre, University of Allahabad, Allahabad 211002, India
[b] Department of Physics, Michigan Technological University, Houghton, MI 49931, USA
[c] Chemistry Division, Bhabha Atomic Research Centre, Trombay, Mumbai 400085, India
[d] Department of Physics and Astronomy, Valparaiso University, Valparaiso, IN 46383, USA
[e] Department of Chemistry, University of Pune, Pune 411007, India
[f] Bundelkhand University, Jhansi, Uttar Pradesh 284128, India

## ARTICLE INFO

## ABSTRACT

The structural evolution and variation of electronic properties of alkaline-earth metal fluoride clusters $(MF_2)_n$ (M = Mg, Ca, Sr, Ba; $n$ = 1–6) are investigated using density functional theory. All these clusters demonstrate ionic-bonding dominated through all sizes considered here, and generally show a preference of 3D structures when $n \geqslant 4$. It is found that the structural evolution of $(MgF_2)_n$ clusters are distinct from the rest of the alkaline-earth clusters owing to the competitive interplay of much smaller ionic radius of Mg and the stronger Mg–F bond. In the ground state configurations, $(MgF_2)_n$ clusters prefer the planar building units, whereas the rest of the $(MF_2)_n$ clusters prefer the 3D building units of a $M_2F_3$ type maximizing the coordination number of the constituent metal atoms. The variations of the binding energy, the ionization potential, the electron affinity and the HOMO–LUMO gap with the cluster size are explained in terms of the change in the ionic radius and the basicity of the constituent metal ions in going from $(MgF_2)_n$ to $(CaF_2)_n$, $(SrF_2)_n$, and $(BaF_2)_n$.

## 1. Introduction

Clusters are the smallest units of matter that can exist stably consisting of a few to a dozen of atoms. Due to the relatively few atoms and the high ratio of under-coordinated atoms, small clusters usually have significantly different structural, physical and chemical properties compared to their bulk counterparts. Extensive efforts consisting of both experiments and theory have been made in the last two decades to study their size-dependent evolutionary properties and, in particular, how their properties converge to corresponding bulk values [1–6]. Interestingly, ionic clusters such as alkali halides, alkaline-earth oxides or alkaline-earth halides are likely to have the bonding characteristics which remain similar throughout all sizes implying that these stoichiometric clusters may have stable bulk-like configurations even at nanoscale. This is due to the fact that an ionic cluster is formed by elements having a large difference in their electronegativity which leads to significant charge transfer between the constituent atoms and dominant electrostatic interactions in the cluster.

Alkaline-earth fluorides are generally known for their intrinsic optical properties and are well-characterized [7–10]. However, this is not the case with small fluoride clusters where only a few studies have attempted to determine their structural and thermochemical properties. The $MgF_2$ monomer was investigated at the level of the coupled cluster theory predicting it to be linear [11]. Also, the calculated binding energy and the effective volume of the global minimum isomers appear to increase almost linearly with the cluster-size for $(MgF_2)_n$ with $n$ = 1–30 [12–14]. It was suggested that $n$ = 8, 10, 13, 15, and 20 are probably the magic numbers for $(MgF_2)_n$ [14]. Also, a comparison of the calculated Raman spectra of $MgF_2$ clusters and the bulk $MgF_2$ with the available experimental data indicated the presence of dangling (terminal) fluorine atoms at the cluster level [15,16].

Despite the expected difference going from $MgF_2$ to $CaF_2$ to $SrF_2$ to $BaF_2$, no attempt has been made to investigate the physical properties of the rest of the fluoride clusters either by theory or experiments. This is what we intend to do in this study with an aim to provide a fundamental understanding of the evolution of structure and properties with the cluster size, and the effect of a variation of the cation within the same group ($Mg^{2+}$ to $Ba^{2+}$) in determining the nature of bonding, and thereby the structural

configurations of the fluoride clusters. In the present paper, we present the results on small clusters of $(MgF_2)_n$, $(CaF_2)_n$, $(SrF_2)_n$ and $(BaF_2)_n$ with $n = 1–6$ obtained using the density function theory (DFT) method.

The details of the computational method are given in Section 2. Results are discussed in Section 3 and a summary of the results is given in Section 4.

## 2. Computational method

Electronic structure calculations on the fluoride clusters were performed in the framework of density functional theory using Gaussian 09 code [17]. The hybrid exchange–correlation functional form B3LYP (i.e. Becke's 3-parameter hybrid exchange functional [18] and Lee, Yang, and Parr correlation functional [19]) was employed. The LanL2DZ [20] and 6-31G* [21] basis sets were used for alkaline-earth metal and fluorine atoms, respectively. The convergence criterion for the maximum force was 0.02 eV/Å and that for the maximum displacement was 0.001 Å. The total energy and density matrix were set to be converged at $3 \times 10^{-5}$ eV and $7 \times 10^{-8}$ e/Å$^3$, respectively.

In order to determine the ground state configurations of $(MF_2)_n$ clusters with M = Mg, Ca, Sr, Ba; $n = 1–6$, a systematic search was performed which consisted of several initial configurations based on symmetry manipulation, similar ionic systems, and fragments from the bulk material. The initial cluster configurations considered for the symmetry-constrained optimization were chosen using a bottom-up approach starting with the monomer, $MF_2$. Both linear and bent configurations were initially constructed for the geometrical optimization. The resulting equilibrium configuration is a completely linear F–M–F configuration for the monomer. On the other hand, the M–F–F linear configuration is significantly higher ($\approx 5$ eV) in energy relative to the F–M–F configuration for all cases. Considering the predicted preference of M–F over F–F bonds, the $(MF_2)_2$ dimers were generated with combinations of two $MF_2$ monomers with M–F bonds and possible symmetry considerations. This approach is then extended for the other fluoride clusters by adding more $MF_2$ monomers. All equilibrium configurations obtained for one series were also used as initial configurations for the other alkaline-earth fluorides. Cleaved bulk fragments were also considered. In this way, we sampled a wide range of configurations including chain-like, ring-like, planar and three-dimensional structures to locate the minimum energy structure for each of the clusters with different composition and size. This approach is similar to what was previously adopted for small-size oxide and nitride clusters studied in our group [3–5]. Furthermore, reliability of our approach is confirmed by so obtained ground-state configurations for $MgF_2$ which are consistent with the reported global minima located by the global optimization basin-hopping (BH) method [14] validating the approach we are using.

## 3. Results and discussion

Figs. 1 and 2 show the ground state configurations of $(MF_2)_n$ ($n = 1–6$) clusters. Some of the representative higher-energy lying isomers of the fluoride clusters are shown in Fig. 3. The relative stability of these isomers is given in Table 1 where zero of the energy is aligned to the total energy of the most stable configuration, referred to as the ground state configuration.

### 3.1. Structural properties

The structural properties together with dissociation energy, fragmentation energy, and cationic Mulliken charge of the ground

state configurations of $(MF_2)_n$ ($n = 1–6$) clusters are given in Table 2.

For the $MF_2$ monomer, the ground state configuration is linear with the M–F bond length of 1.72, 2.06, 2.20, 2.33 Å for $MgF_2$, $CaF_2$, $SrF_2$, and $BaF_2$, respectively. The Mg–F bond length of the $MgF_2$ monomer is found to be slightly shorter than the previous values reported at the CCSD(T)/awCVTZ level ($R_{Mg-F} = 1.742$ Å) [11], the MP2/TZV(3d1f) level ($R_{Mg-F} = 1.761$ Å) and MP4/TZV(3d1f) level ($R_{Mg-F} = 1.763$ Å) [12] of theory. The increase in M–F bond length can be attributed to increase in the cationic size in going from Mg to Ba. On the other hand, the cationic Mulliken charge slightly increases from $1.3e$ for $MgF_2$ to $1.7e$ for $BaF_2$ due to the increased basicity of the cation. As a result, the metal–fluorine bond is relatively strong in $MgF_2$ compared to that in $BaF_2$.

A dimerization of $MF_2$ unit brings the differences between $(MgF_2)_2$ and the other members of the fluorides. The clusters, except $(MgF_2)_2$, show a capped trigonal structure with $C_{3v}$ symmetry – the smallest 3D unit in which two metal cations are bridged via three F ions in their ground state configurations (Fig. 2). The $(MgF_2)_2$ cluster, however, favors a planar structure with $D_{2h}$ symmetry. It has two bridging F ions between two Mg cations. The non-planar $C_{3v}$ isomer is higher in energy ($\approx 0.63$ eV) relative to the planar $D_{2h}$ isomer (Table 1).

For $n = 3$, the difference between $(MgF_2)_3$ with the other fluoride clusters persist; $(MgF_2)_3$ prefers a planar $D_{2d}$ structure whereas the other $(MF_2)_3$ clusters prefer a $C_{2v}$ structure formed by a triangular metal frame, capped by fluorine ions. In these 3D structures, between each pair of cations, we find three bridging F ions. It is worth mentioning that the average Mg–F bond length for $D_{2h}$ and $D_{2d}$ structures of $(MgF_2)_2$ and $(MgF_2)_3$ are in good agreement with the values obtained previously at MP2/TZV level of Theory [13].

The $(MF_2)_4$ clusters seem to prefer low-symmetry $C_s$ structures over $C_{3v}$ or $D_{4h}$ structures (Table 1). In the ground state configurations of the $(MF_2)_4$ clusters, except for $(MgF_2)_4$, the metallic cations frame forms a rhombus capped by fluorine ions leading to the coordination number of the cation to be four or five. On the other hand, $(MgF_2)_4$ is consisted of the $Mg_2F_2$ planar unit with a relative large metal–metal distance and the coordination number of three or four for cations (Fig. 1).

In line with the tetramer unit of $(MF_2)_n$, the relative low-symmetry $C_1$ or Cs structures are found to be the ground state configurations for $(MF_2)_5$ and $(MF_2)_6$ clusters. Interestingly, $(MgF_2)_5$ and $(MgF_2)_6$ clusters consistently show a preference for different ground state configurations; $(MgF_2)_5$ prefers $C_s$ configuration, and $(MgF_2)_6$ prefers $C_2$ configuration. Note that the energy of the $C_1$-(i) configuration preferred by the other $(MF_2)_5$ clusters is 0.4 eV higher than the calculated ground state $C_s$ configuration of $(MgF_2)_5$ (Table 1).

The predicted ground state configurations of $(MF_2)_n$ clusters appear to favor heteroatomic bonds over homoatomic bonds, the same as found in the bulk. However, the calculated GGA-DFT results find a subtle difference between $(MgF_2)_n$ and the rest of the fluoride clusters; $(CaF_2)_n$, $(SrF_2)_n$ and $(BaF_2)_n$ prefer a 3D building unit, while $(MgF_2)_n$ prefers a 2D building unit (Figs. 1 and 2). This difference is likely due to the much smaller radius of Mg as compared to the other alkaline-earth cations leading to energetic considerations when one brings in more anions near to each other in a given cluster configuration. The penalty due to electrostatic repulsion between fluorine ions is higher than the gain in energy by electrostatic attraction between Mg and F ions in the $(MgF_2)_n$ cluster. Note that the relatively small radius of Mg also explains why $MgF_2$ bulk has a rutile phase at ambient conditions. In the rutile phase, the coordination number of Mg with F is 6, whereas in the fluorite phase, the coordination number of metal with F is 8 [22]. Thus, distinctly different geometrical structures of the $(MgF_2)_n$ clusters relative to the other $(MF_2)_n$ clusters appears to
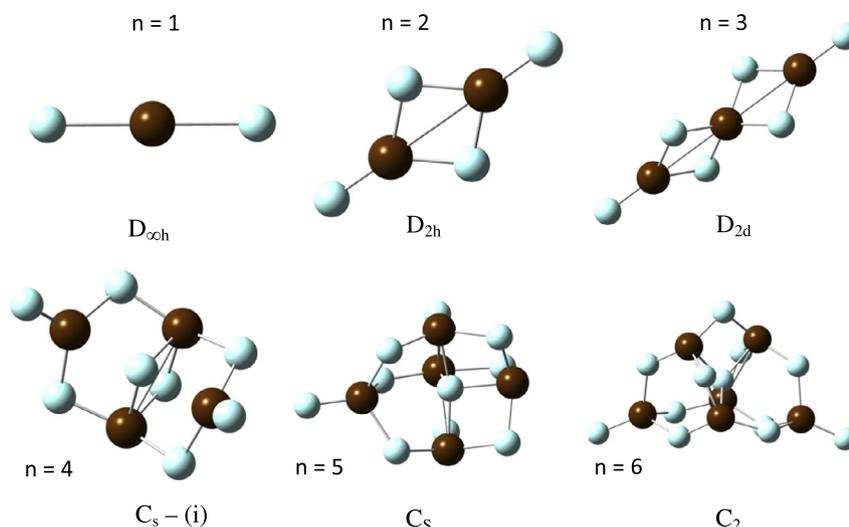
**Fig. 1.** The ground state configurations of $(MgF_2)_n$ ($n$ = 1–6) clusters. Symbols: M in brown; F in cyan. (For interpretation of the references to colour in this figure legend, the reader is referred to the web version of this article.)



**Fig. 2.** The ground state configurations of $(MF_2)_n$ (M = Ca, Sr, Ba; $n$ = 1–6) clusters. Symbols: M in brown; F in cyan. (For interpretation of the references to color in this figure legend, the reader is referred to the web version of this article.)
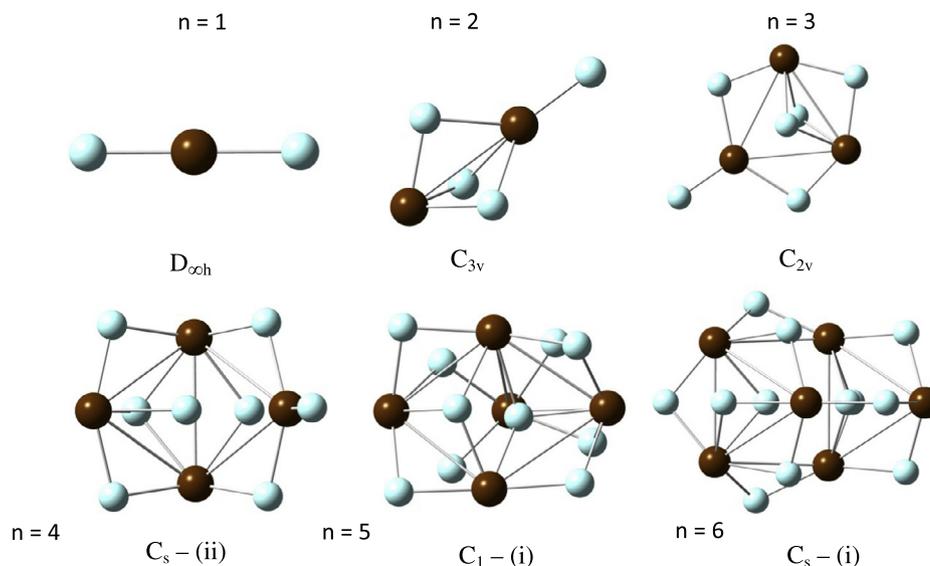
be a direct reflection of the difference observed in the corresponding bulk fluorides.

### 3.2. Stability

The stability of the small fluoride clusters is examined via calculations of the dissociation and fragmentation energy. The dissociation energy is taken to be average heat of formation of a cluster from its constituent ions and is given by

$$E_{diss} = [E((MF_2)_n) - nE(M^{2+}) - 2nE(F^-)]/3n \qquad (1)$$

where $E((MF_2)_n)$, $E(M^{2+})$ and $E(F^-)$ are the total energy of the cluster, the energy of a metal cation and the energy of a fluorine ion, respectively. The calculated dissociation energy for $MgF_2$ monomer agrees well with previous studies where 30.29 eV per $MgF_2$ unit was found at the MP2/TZV(3d1f) level of theory [12].

In general, the dissociation energy increases rapidly for ($n$ = 2, 3) clusters and then follows a gradual increase as the cluster size grows with small humps or dips for specific sizes indicating changes in their relative stabilities. These observations are in

agreement with the previous study by Francisco et al. [13] performed at the MP2/TZV(1d) level of theory in which the energy required to dissociate the $(MgF_2)_n$ cluster into its constituent ions increases from 27.71 to 29.06, 29.53 eV per $MgF_2$ unit when the cluster size $n$ increases from 1 to 2, 3, respectively. In addition, for a given $n$, the dissociation energy per unit formula ($E_{diss}$) is higher for $(MgF_2)_n$ than for $(BaF_2)_n$ (Table 2). This is simply reflective of the fact that the metal–F bonds in $MgF_2$ are shorter and stronger than the other alkaline-earth metal–F bonds in the clusters considered. In addition, the values of dissociation energy are comparable to the cohesive energies measured for the bulk materials, which are 30.19, 27.04, and 24.26 eV per $MF_2$ unit for $MgF_2$, $CaF_2$, and $BaF_2$, respectively.

In order to study the relative stability, it is more instructive to analyze the first derivative of the total energy, i.e., the fragmentation energy which is defined as the energy required to remove a $MF_2$ unit from a $(MF_2)_n$ cluster.

$$E_{fragmentation} = E((MF_2)_{n-1}) + E(MF_2) - E((MF_2)_n) \qquad (2)$$

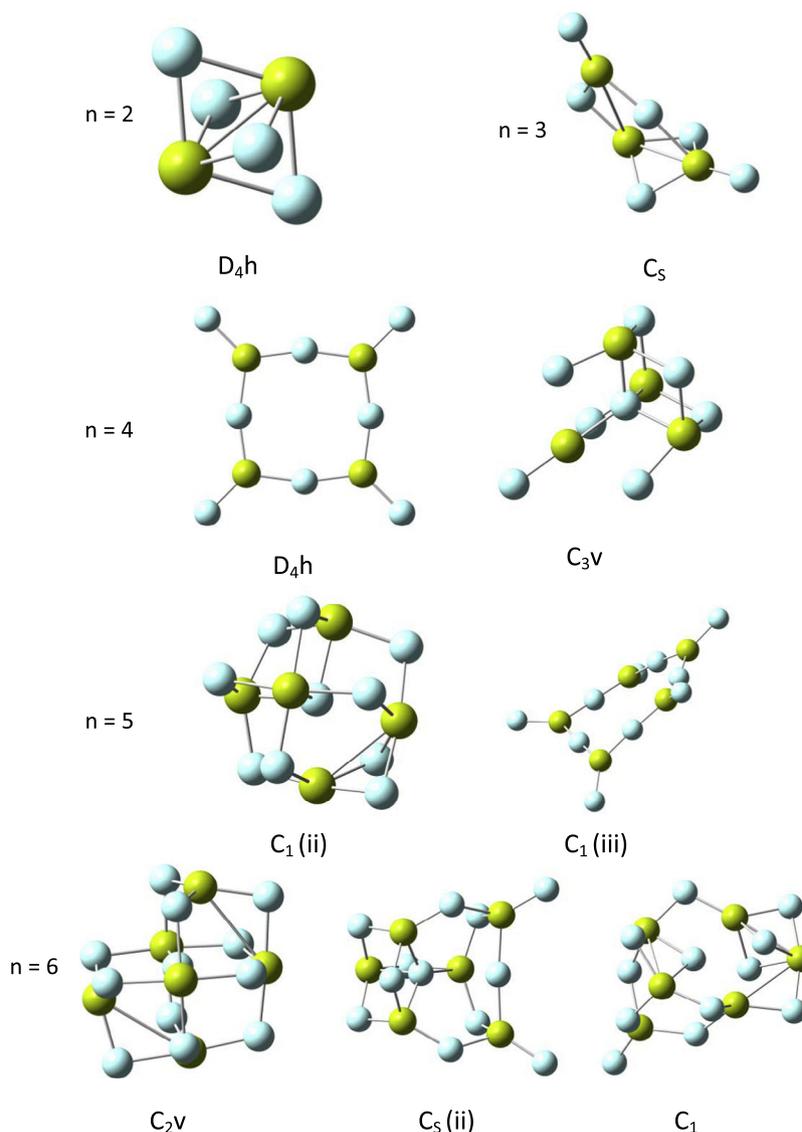where $E(MF_2)_n$ is the total energy of the $(MF_2)_n$ cluster.

**Fig. 3.** Some of the higher-energy isomeric configurations of the $(MF_2)_n$ ($n$ = 1–6) clusters considered (Table 1). Symbols: M in green; F in cyan. (For interpretation of the references to color in this figure legend, the reader is referred to the web version of this article.)

Table 2 shows that the fragmentation energy of the $(MF_2)_n$ clusters increases with the increase in the cluster size suggesting the stability of the larger $(MF_2)_n$ cluster. These results again agree with the report by Francisco et al. [14] where they found that binding energy per $MgF_2$ unit increases with cluster size, which means that higher values will be required to dissociate them. Note that the values of the fragmentation energy for $(MgF_2)_n$ clusters are lower than those for the other fluoride clusters. This observation is in line with the fact that Mg has a lower coordination number with F and the enclosing of more $MgF_2$ units does not result in a higher stabilization relative to the other fluoride clusters. Furthermore, $(MgF_2)_n$ clusters show a higher tolerance for the M–F dangling bonds in which F is only coordinated to a metal ion. This fact also accounts for the lower fragmentation energy associated with $(MgF_2)_n$ clusters.

We now search for the magic clusters in the $(MF_2)_n$ series by calculating the second energy difference in energy ($\Delta^2 E$), though our cluster-size considered is somewhat limited. $\Delta^2 E$ is calculated as

$$\Delta^2 E = 2E((MF_2)_n) - E((MF_2)_{n+1}) - E((MF_2)_{n-1}) \qquad (3)$$

where $E(MF_2)_n$ is the total energy of the $(MF_2)_n$ cluster.

Fig. 4 displays the variation of $\Delta^2 E$ as a function of cluster size for $(MF_2)_n$ clusters. Note that Eq. (3) suggests that the clusters with

the negative value of $\Delta^2 E$ are more stable than their nearest neighbors. Thus, $n$ = 4 appears to be the magic number only for the $(MgF_2)_n$ and $(CaF_2)_n$ clusters.

Frequency calculations were carried out for the ground state configurations for each of the composition and cluster size. The higher frequency region represents the stretching mode associated with metal–fluorine bonds with the highest vibrational frequency being ~800, 530, 450 and 380 cm$^{-1}$ for larger clusters of $MgF_2$, $CaF_2$, $SrF_2$, and $BaF_2$, respectively. The predicted values of the stretching mode further confirms the strength of metal–fluorine bond which is the strongest in $MgF_2$ and decreases as one moves down in the periodic group from Mg to Ca to Sr to Ba. These calculated frequencies for small clusters are higher than the maximal vibrational frequencies for the bulk counterparts, which are ~625, 463, 374 and 326 cm$^{-1}$ for $MgF_2$, $CaF_2$, $SrF_2$, and $BaF_2$, respectively [23,24].

### 3.3. Electronic structure

After establishing the stability and the ground state configurations of the $(MF_2)_n$ clusters, we now analyze their electronic properties via the nature of the highest occupied molecular orbital

**Table 1**
Symmetries and energies of the isomeric configurations relative to the ground state configuration for $(MF_2)_n$ (M = Mg, Ca, Sr, Ba; $n$ = 1–6) clusters. The representative configurations are given in Figs. 1–3.

| Cluster | Symmetry | Relative energy (eV) | | | |
|---|---|---|---|---|---|
| | | M = Mg | M = Ca | M = Sr | M = Ba |
| $MF_2$ | $D_{\infty h}$ | 0 | 0 | 0 | 0 |
| $(MF_2)_2$ | $D_{2h}$ | 0 | 0.04 | 0.24 | 0.32 |
| | $C_{3v}$ | 0.63 | 0 | 0 | 0 |
| | $D_{4h}$ | 3.34 | 1.26 | 0.80 | 0.59 |
| $(MF_2)_3$ | $D_{2d}$ | 0 | 0.99 | 1.30 | 1.41 |
| | $C_{2v}$ | 0.50 | 0 | 0 | 0 |
| | $C_s$ | 0.27 | 0.84 | 1.02 | 1.09 |
| $(MF_2)_4$ | $C_s$-(i) | 0 | 0.75 | 1.01 | 1.10 |
| | $C_s$-(ii) | 0.54 | 0 | 0 | 0 |
| | $C_{3v}$ | 1.55 | 0.71 | 0.64 | 0.62 |
| | $D_{4h}$ | 2.52 | 4.22 | 4.50 | 4.45 |
| $(MF_2)_5$ | $C_s$ | 0 | 0.51 | 0.69 | 1.03 |
| | $C_1$-(i) | 0.44 | 0 | 0 | 0 |
| | $C_1$-(ii) | 0.97 | 0.90 | 1.03 | 1.36 |
| | $C_1$-(iii) | 4.22 | 6.88 | 7.26 | 7.42 |
| $(MF_2)_6$ | $C_2$ | 0 | 1.97 | 2.46 | 2.65 |
| | $C_s$-(i) | 0.91 | 0 | 0 | 0 |
| | $C_s$-(ii) | 0.16 | 2.07 | 2.46 | 2.51 |
| | $C_{2v}$ | 0.19 | 0.60 | 0.78 | 0.88 |
| | $C_1$ | 0.60 | 0.93 | 1.15 | 0.97 |

(HOMO) and the lowest unoccupied molecular orbital (LUMO), magnitude of the HOMO–LUMO gap, the ionization potential (IP) and the electron affinity (EA).

The ionization potential (IP) and electron affinity (EA) for the ground state configuration of $(MF_2)_n$ clusters are computed as follows [5]:

$$IP = E_{q=+1} - E_{q=0} \qquad (4)$$

$$EA = E_{q=0} - E_{q=-1} \qquad (5)$$

**Table 2**
The ground state configurations of $(MF_2)_n$ (M = Mg, Ca, Sr, Ba; $n$ = 1–6) clusters: (average) bond length (($R_{M-F}$), dissociation energy ($E_{diss.}$), Fragmentation energy ($E_{frag.}$), and cationic Mulliken charge ($Q_{cat.}$). The (vertical) ionization potential (IP), (vertical) electron affinity (EA), and the HOMO–LUMO gap (H–L) of $(MF_2)_n$ clusters calculated at the GGA-DFT level of theory.

| Cluster | $R_{(M-F)}$ (Å) | $E_{diss.}$ (eV) | $E_{frag.}$ (eV) | $Q_{cat.}$ (e) | IP (eV) | EA (eV) | $E_{H-L}$ (eV) |
|---|---|---|---|---|---|---|---|
| $MgF_2$ | 1.72 | −10.1 | – | 1.3 | 12.1 | −0.5 | 7.4 |
| $(MgF_2)_2$ | 1.84 | −10.7 | 3.6 | 1.3 | 11.5 | −0.4 | 7.5 |
| $(MgF_2)_3$ | 1.86 | −10.9 | 3.5 | 1.3 | 11.3 | −0.4 | 7.6 |
| $(MgF_2)_4$ | 1.87 | −11.1 | 4.7 | 1.3 | 10.8 | 0.8 | 4.8 |
| $(MgF_2)_5$ | 1.88 | −11.2 | 4.1 | 1.3 | 10.5 | 0.7 | 5.0 |
| $(MgF_2)_6$ | 1.89 | −11.2 | 4.3 | 1.3 | 10.1 | 0.9 | 5.2 |
| $CaF_2$ | 2.06 | −8.2 | – | 1.5 | 10.0 | ≈0.0 | 5.1 |
| $(CaF_2)_2$ | 2.2 | −8.8 | 4.0 | 1.5 | 9.3 | 1.6 | 2.7 |
| $(CaF_2)_3$ | 2.24 | −9.2 | 4.8 | 1.4 | 8.9 | 1.1 | 3.0 |
| $(CaF_2)_4$ | 2.24 | −9.4 | 5.7 | 1.4 | 8.9 | 1.1 | 2.8 |
| $(CaF_2)_5$ | 2.25 | −9.5 | 5.4 | 1.4 | 9.5 | 0.3 | 6.2 |
| $(CaF_2)_6$ | 2.26 | −9.6 | 6.1 | 1.4 | 9.4 | 0.5 | 5.8 |
| $SrF_2$ | 2.2 | −7.6 | – | 1.6 | 9.0 | 0.1 | 4.3 |
| $(SrF_2)_2$ | 2.31 | −8.2 | 3.9 | 1.5 | 10.2 | 1.4 | 2.3 |
| $(SrF_2)_3$ | 2.38 | −8.5 | 4.7 | 1.5 | 8.8 | 0.3 | 2.6 |
| $(SrF_2)_4$ | 2.37 | −8.7 | 5.6 | 1.5 | 8.2 | 1.0 | 2.6 |
| $(SrF_2)_5$ | 2.39 | −8.9 | 5.4 | 1.5 | 8.4 | 0.5 | 5.1 |
| $(SrF_2)_6$ | 2.41 | −8.9 | 6.1 | 1.5 | 8.7 | 0.5 | 5.3 |
| $BaF_2$ | 2.33 | −7.0 | – | 1.7 | 8.1 | 0.1 | 3.6 |
| $(BaF_2)_2$ | 2.47 | −7.6 | 3.7 | 1.6 | 7.7 | 1.2 | 2.1 |
| $(BaF_2)_3$ | 2.52 | −7.9 | 4.5 | 1.7 | 7.4 | 0.9 | 2.4 |
| $(BaF_2)_4$ | 2.51 | −8.1 | 5.3 | 1.6 | 7.4 | 0.8 | 2.4 |
| $(BaF_2)_5$ | 2.5 | −8.2 | 5.5 | 1.5 | 7.7 | 0.3 | 4.4 |
| $(BaF_2)_6$ | 2.55 | −8.3 | 5.6 | 1.6 | 7.9 | 0.3 | 4.6 |
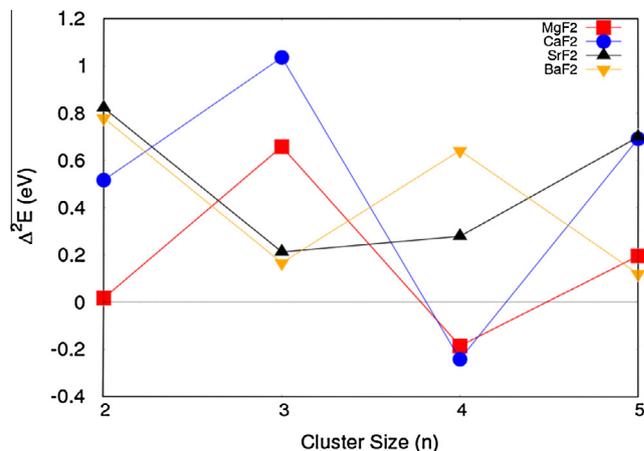


**Fig. 4.** The second energy difference in energy ($\Delta^2 E$) versus size ($n$) of $(MF_2)_n$.

where $E$ is the total energy of a cluster and $q$ denotes its charge. We use the vertical approximation to calculate both IP and EA of a given cluster. The vertical electron affinity (VEA) is defined as energy difference between the anionic and neutral cluster when both are at the ground state configuration of the neutral ($q = 0$) cluster. The vertical ionization potential (VIP) is defined as the energy difference between the cationic and neutral clusters, both at the ground state configuration of the neutral ($q = 0$) cluster.

Table 2 collects IP and EA values together with the HOMO–LUMO gap for $(MF_2)_n$ clusters. From the stability point of view, a cluster will be electronically stable if it is resistant to donate any electron from HOMO (reflected by its IP values) and do not want to accept any electron in its LUMO (reflected in EA values). To satisfy these stability criterions, the cluster must have higher ionization potential as well as very low electron affinity. In the present study, the higher ionization energy and the lower electron affinity of all these clusters corroborated their electronic stability/lower reactivity (Table 2). The higher electronic stability of these clusters is also reflected in their large HOMO–LUMO gap which is also termed as global hardness, $\eta$. The results also show that Mg series clusters have highest ionization potential and a large HOMO–LUMO gap. The IP values decrease in going from $MgF_2$ to $BaF_2$ for a given cluster-size, indicating higher electronic stability of $MgF_2$ cluster in comparison to others. Interestingly, we find the negative values for the electron affinity for $MgF_2$ clusters with $n < 4$, indicating very high electronic stability of the system against the addition of an electron. A higher strength of Mg–F bond together with the well-balanced charge state results in very high stability of the smaller $MgF_2$ cluster and any addition or deficiency of electrons leads to relative destabilization of system. The EA values are, however, all positive for $CaF_2$, $SrF_2$, and $BaF_2$ clusters with the highest value for the $n = 2$ cluster indicating the highest electron affinity among the $n \leqslant 6$ clusters.

The HOMO and LUMO orbitals of $(MF_2)_1$ and $(MF_2)_6$ clusters are plotted in Fig. 5. The dominant contribution to HOMO for $(MgF_2)_n$ and $(CaF_2)_n$ appears from the F-$p$ orbitals, though contributions from cationic-$p$ orbitals appear for $(SrF_2)_n$ and $(BaF_2)_n$. These features corroborate the high IP values for $(MgF_2)_n$ and $(CaF_2)_n$ clusters, as fluorine is a highly electronegative element and it is very difficult to extract an electron from HOMO consisting of $p$ orbitals of fluorine. On the other hand, cationic orbitals form the LUMO of the fluoride clusters considered. A low electronegativity nature (or highly electro-positive nature) of cations, results in a poor electron acceptability in cation $s$ orbitals and hence lower electron affinity values of the fluoride clusters.

In order to understand the distinct nature of $(MgF_2)$, we compare its bonding features with that of $(CaF_2)$ based on the Bader
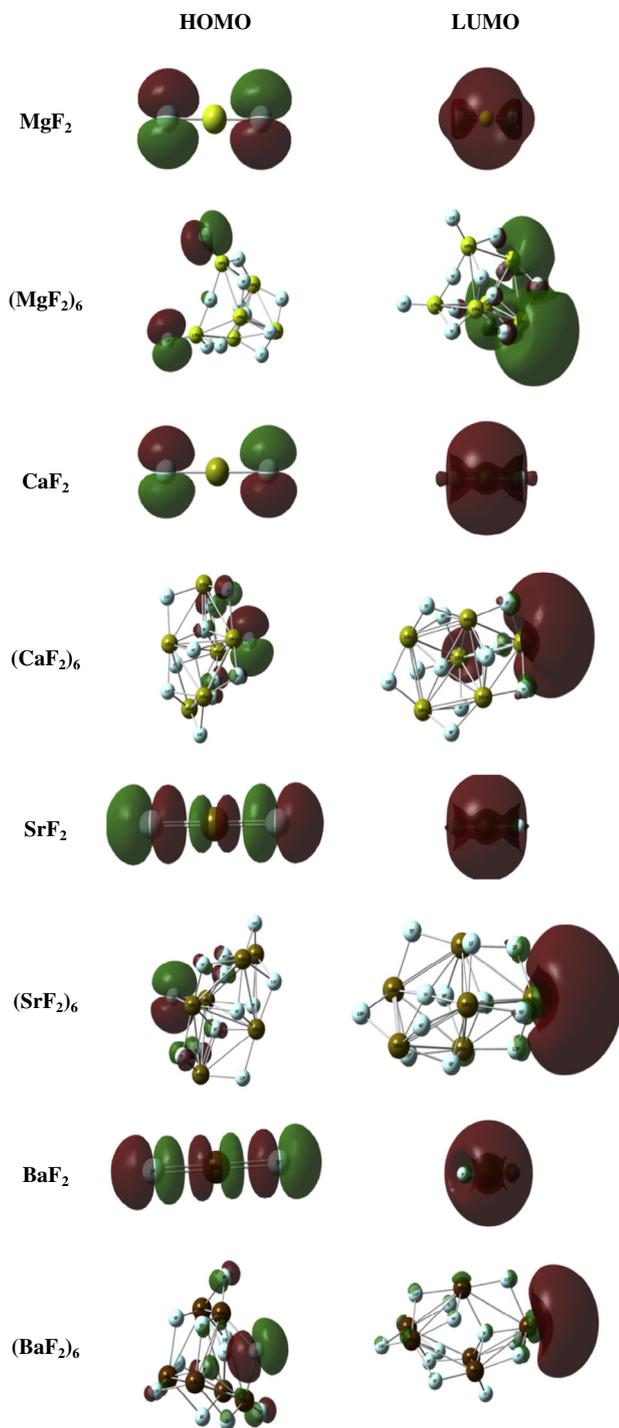
**Fig. 5.** Molecular orbitals of $(MF_2)_1$ and $(MF_2)_6$ clusters with M = Mg, Ca, Sr, and Ba.



**Fig. 6.** The calculated AIM parameters of $(MgF_2)$ and $(CaF_2)$: $\rho$ and $(\nabla^2\rho)$ in a.u. The atoms are shown by big spheres and the bond critical points (BCPs) by small spheres. The radii of atoms are not according to scale.

Fig. 6 shows that the electron density BCPs are located at 0.783 and 1.049 Å, respectively from the corresponding metal atoms of $(MgF_2)$ and $(CaF_2)$ clusters [30] for the detailed results of AIM parameters). The calculated value of $\rho(\nabla^2\rho)$ for the Mg–F bond is 0.0902 a.u. (0.8376 a.u.) as compared to that of 0.0627 a.u. (0.4809 a.u.) for the Ca-F bond. Therefore, the Mg–F bond appears to be relatively strong and ionic as compared to the Ca–F bond. On the other hand, the covalent bond orders are calculated to be 0.30 and 0.35 for Mg–F and Ca–F bonds, respectively. A slightly higher delocalization of electrons is seen for the Ca–F bond, which is in line with the higher degree of hybridization of metal-$p$ orbitals and F-$p$ orbitals (see HOMOs in Fig. 5).

## 4. Summary

In the present study, the size-dependent structural, electronic and vibrational properties of small clusters of the alkaline-earth metal fluorides (i.e. $(MF_2)_n$ (M = Mg, Ca, Sr, Ba, $n = 1$–6)) were investigated in the framework of density functional theory. A distinct nature of the $(MgF_2)_n$ clusters in terms of structural evolution is predicted as compared to other alkaline-earth fluoride clusters. It is likely due to the competitive interplay of the stronger Mg–F bonds and the relative small radius of Mg ions. In the ground state configurations, $(MgF_2)_n$ clusters prefer the planar building units, whereas the rest of the $(MF_2)_n$ clusters prefer the 3D building units of a $M_2F_3$ type maximizing the coordination number of metal atoms. But all of them show a preference of 3D structures when $n \geqslant 4$ towards the bulk-like structures. The $(MgF_2)_n$ clusters are also featured by much higher dissociation energy, higher vibrational frequencies, higher ionization energy, lower electron affinity and higher HOMO–LUMO gap, as a reflection of their stronger ionic-dominated bonding. The $(MF_2)_n$ (M = Ca, Sr, Ba) series, on the other hand, show general similarity in their most-stable structure, energetics and features of electronic structure, while maintaining a systematic variation in these properties in accordance with the change of the basicity and size of the alkaline-earth metal going from Ca to Sr to Ba. As is common to all the $(MF_2)_n$ clusters, the stability of the cluster increases with the size with its binding energy approaching that of the bulk counterpart.

Atoms in Molecule (AIM) theory [25]. It has been shown that topographical parameters *viz.* the electron density $\rho$ at the corresponding (3, −1) bond critical point (BCP) and its Laplacian ($\nabla^2\rho$) are connected with the bonding properties. The sign of $\nabla^2\rho$ indicates that the electronic charge is concentrated (negative value) or locally depleted (positive value), corresponding to the covalent (sharing of electrons) or ionic/electrostatic (closed shell) interactions respectively [26–31]. Note that the electron density topographical parameters are calculated using both the LanL2DZ set for alkaline-earth metal atoms and the 6-31G* basis set for fluorine atoms in the fluoride clusters considered.
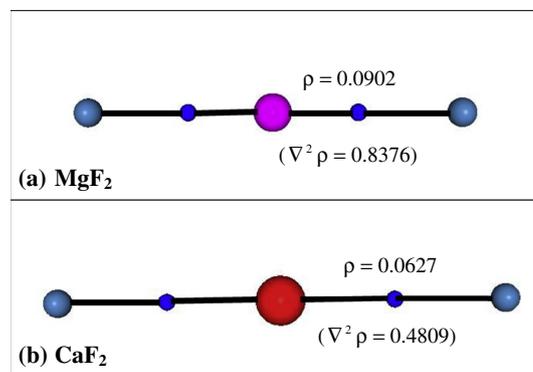
computing cluster at Michigan Technological University, was used in obtaining results presented in this publication.

## Appendix A. Supplementary material

Supplementary data associated with this article can be found, in the online version, at http://dx.doi.org/10.1016/j.comptc.2014.05.007.

## References

[1] T.P. Martin, U. Näher, H. Göhlich, T. Lange, "The geometric shell structure of metal clusters." Physics and Chemistry of Finite Systems: From Clusters to Crystals, in: P. Jena, S.N. Khanna, B.K. Rao (Eds.), NATO ASI Series, Springer, Germany, 1998, pp. 147–156.
[2] T.P. Martin, Metal halide clusters, Ber. Bunsenges. Phys. Chem. 88 (1984) 300–302.
[3] J.M. Recio, R. Pandey, A. Ayuela, A.B. Kunz, Molecular orbital calculations on $(MgO)_n$ and $(MgO)_n^+$ clusters ($n = 1$–13), J. Chem. Phys. 98 (1993) 4783.
[4] A.K. Kandalam, M.A. Blanco, R. Pandey, theoretical study of AlnNn, GanNn, And InnNn ($n = 4, 5, 6$) Clusters, J. Phys. Chem. B 106 (2002) 1945–1953.
[5] A. Costales, M.A. Blanco, E. Francisco, A.M. Pendás, R. Pandey, First principles study of neutral and anionic (Medium-Size) aluminum nitride clusters: AlnNn, N = 7–16, J. Phys. Chem. B 110 (2006) 4092–4098.
[6] M.A. Duncan, Advances in metal and semiconductor clusters, Cluster Materials, vol. 4, Elsevier, 1998.
[7] M. Pang, D. Liu, Y. Lei, S. Song, J. Feng, W. Fan, H. Zhang, Rare-earth-doped bifunctional alkaline-earth metal fluoride nanocrystals via a facile microwave-assisted process, Inorg. Chem. 50 (2011) 5327–5329.
[8] J. Vail, E. Emberly, T. Lu, M. Gu, R. Pandey, Simulation of point defects in high-density luminescent crystals: oxygen in barium fluoride, Phys. Rev. B 57 (1998) 764–772.
[9] H. Jiang, R. Pandey, C. Darrigan, M. Rérat, First-principles study of structural, electronic and optical properties of BaF2 in its cubic, orthorhombic and hexagonal phases, J. Phys.: Conden. Matter 15 (2003) 709–718.
[10] E. Cadelano, G. Cappellini, Electronic structure of fluorides: general trends for ground and excited state properties, Eur. Phys. J. B 81 (2011) 115–120.
[11] M. Vasiliu, D. Feller, J.L. Gole, D.A. Dixon, Structures and heats of formation of simple alkaline earth metal compounds: fluorides, chlorides, oxides, and hydroxides for Be, Mg, and Ca, J. Phys. Chem. A 114 (2010) 9349–9358.
[12] E. Francisco, A. Costales, A.M. Pendás, Structure and bonding in magnesium difluoride clusters: the MgF molecule, J. Phys. Chem. A 105 (2001) 4126–4135.
[13] E. Francisco, A.M. Pendás, A. Costales, Structure and bonding in magnesium difluoride clusters: the $(MgF_2)_n$ ($n = 2$–3) Clusters, J. Phys. Chem. A 106 (2002) 335–344.
[14] E. Francisco, A.M. Pendás, M. Blanco, Global optimization of ionic $Mg_{(n)}F_{(2n)}$ ($n = 1$–30) clusters, J. Chem. Phys. 123 (2005) 234305.
[15] S. Neelamraju, J.C. Schön, K. Doll, M. Jansen, Ab initio and empirical energy landscapes of $(MgF_2)n$ clusters ($n = 3,4$), Phys. Chem. Chem. Phys. 14 (2012) 1223–1234.
[16] S. Neelamraju, A. Bach, J. Schön, D. Fischer, M. Jansen, Experimental and theoretical study on Raman spectra of magnesium fluoride clusters and solids, J. Chem. Phys. 137 (2012) 194319.
[17] Gaussian 09, Revision B.01, M.J. Frisch, G.W. Trucks, H.B. Schlegel, G.E. Scuseria, M.A. Robb, J.R. Cheeseman, G. Scalmani, V. Barone, B. Mennucci, G.A. Petersson, H. Nakatsuji, M. Caricato, X. Li, H.P. Hratchian, A.F. Izmaylov, J. Bloino, G. Zheng, J.L. Sonnenberg, M. Hada, M. Ehara, K. Toyota, R. Fukuda, J. Hasegawa, M. Ishida, T. Nakajima, Y. Honda, O. Kitao, H. Nakai, T. Vreven, J.A. Montgomery Jr., J.E. Peralta, F. Ogliaro, M. Bearpark, J.J. Heyd, E. Brothers, K.N. Kudin, V.N. Staroverov, R. Kobayashi, J. Normand, K. Raghavachari, A. Rendell, J.C. Burant, S.S. Iyengar, J. Tomasi, M. Cossi, N. Rega, N.J. Millam, M. Klene, J.E. Knox, J.B. Cross, V. Bakken, C. Adamo, J. Jaramillo, R. Gomperts, R.E. Stratmann, O. Yazyev, A.J. Austin, R. Cammi, C. Pomelli, J.W. Ochterski, R.L. Martin, K. Morokuma, V.G. Zakrzewski, G.A. Voth, P. Salvador, J.J. Dannenberg, S. Dapprich, A.D. Daniels, Ö. Farkas, J.B. Foresman, J.V. Ortiz, J. Cioslowski, D.J. Fox, Gaussian Inc, Wallingford CT, 2009.
[18] A.D. Becke, Density-functional thermochemistry. III. The role of exact exchange, J. Chem. Phys. 98 (1993) 5648.
[19] C. Lee, W. Yang, R.G. Parr, Development of the Colle-Salvetti correlation-energy formula into a functional of the electron density, Phys. Rev. B 37 (2) (1988) 785.
[20] P.J. Hay, W.R. Wadt, Abinitio effective core potentials for molecular calculations. Potentials for the transition metal atoms Sc to Hg, J. Chem. Phys. 82 (1985) 270.
[21] V.A. Rassolov, M.A. Ratner, J.A. Pople, P.C. Redfern, L.A. Curtiss, 6-31G* basis set for third-row atoms, J. Comput. Chem. 22 (9) (2001) 976–984.
[22] W.E. Addison, Structural Principles in Inorganic Compounds, John Wiley & Sons, Inc., New York, 1961.
[23] S.P.S. Portq, P.A. Fleury, T.C. Damen, Phys. Rev. 154 (1967) 522.
[24] W. Kaiser, W.G. Spitzer, R.H. Kaiser, L.E. Howarth, Phys. Rev. 127 (1962) 1950.
[25] R.F.W. Bader, Atoms in Molecules-A Quantum Theory, Oxford University Press, Oxford, U.K, 1990.
[26] R.F.W. Bader, A bond path: a universal indicator of bonded interactions, J. Phys. Chem. A 102 (1998) 7314–7323.
[27] U. Koch, P.L.A. Popelier, Characterization of C–H–O hydrogen bonds on the basis of the charge density, J. Phys. Chem. 99 (1995) 9747–9754.
[28] T.K. Krygowski, B.T. Stepień, Sigma- and Pi-electron delocalization: focus on substituent effects, Chem. Rev. 105 (2005) 3482–3512.
[29] L. Sobczyk, S.J. Grabowski, T.M. Krygowski, Interrelation between H-bond and Pi-electron delocalization, Chem. Rev. 105 (2005) 3513–3560.
[30] R.I. Zubatyuk, O.V. Shishkin, L. Gorb, J. Leszczynski, Homonuclear versus heteronuclear resonance-assisted hydrogen bonds: tautomerism, aromaticity, and intramolecular hydrogen bonding in heterocyclic systems with different exocyclic proton donor/acceptor, J. Phys. Chem. A 113 (2009) 2943–2952.
[31] Z. Jamshidi, M.F. Far, University of Cagliari, "Binding of Noble Metal Clusters with Rare Gas Atoms: Theoretical Investigation", J. Phys. Chem. A 116 (2012) 12510–12517.